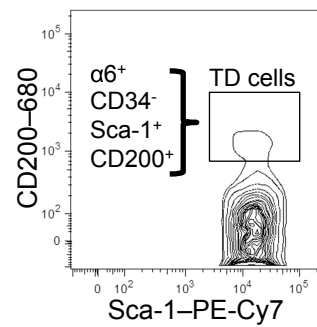
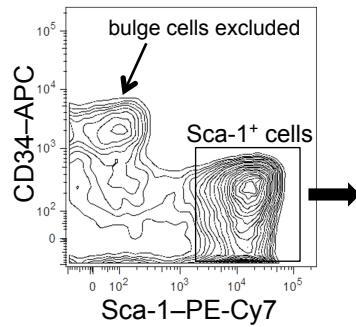
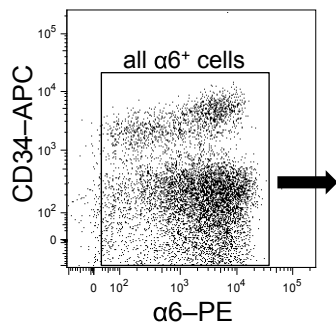
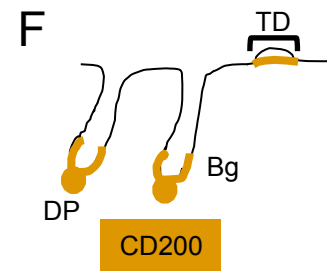
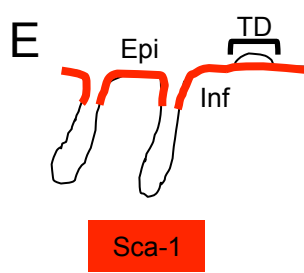
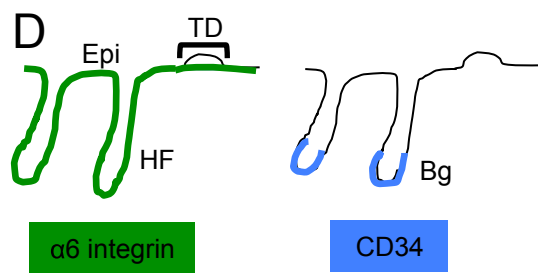
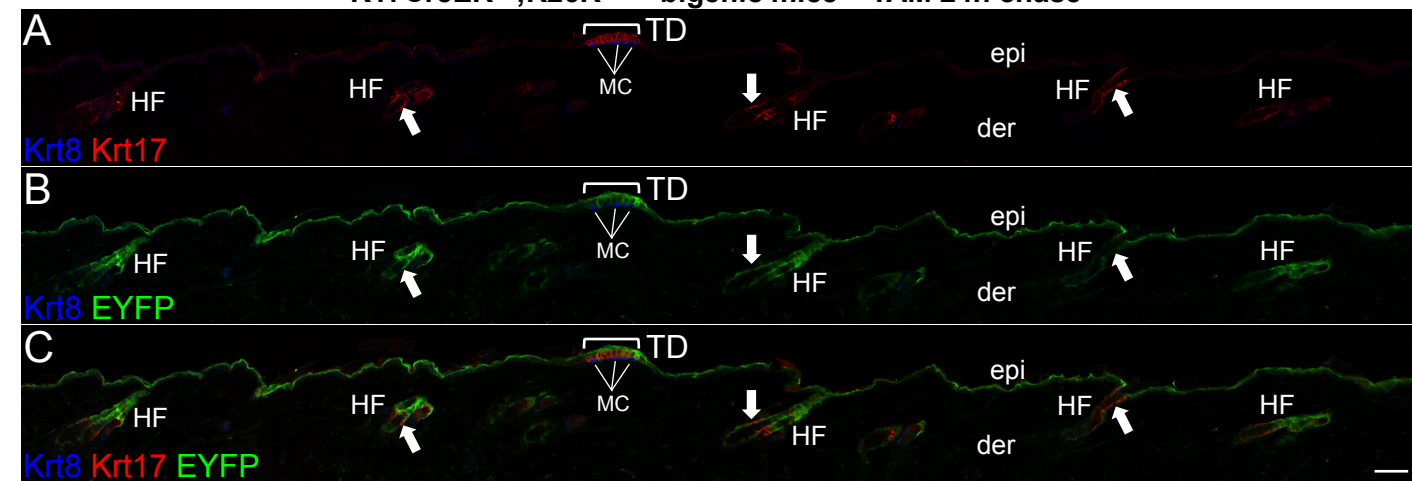
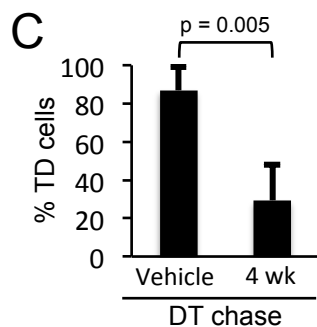
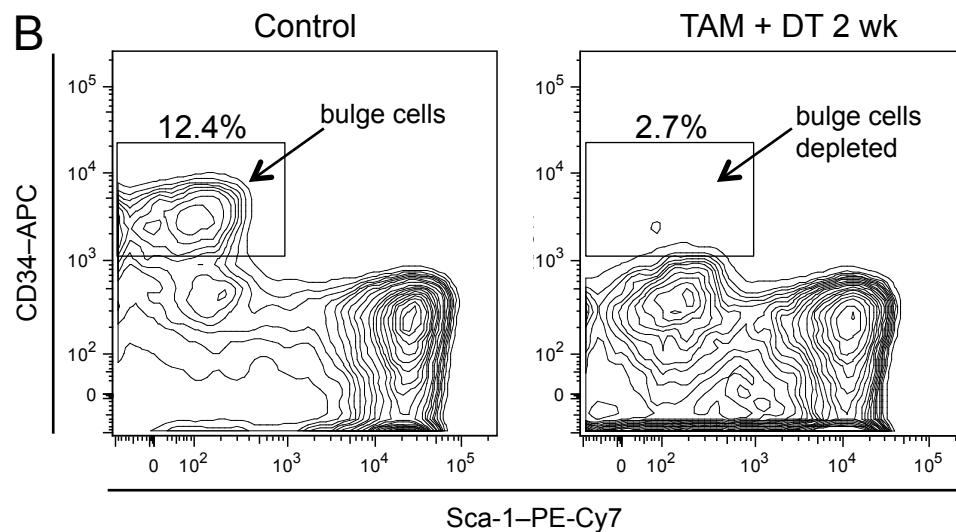
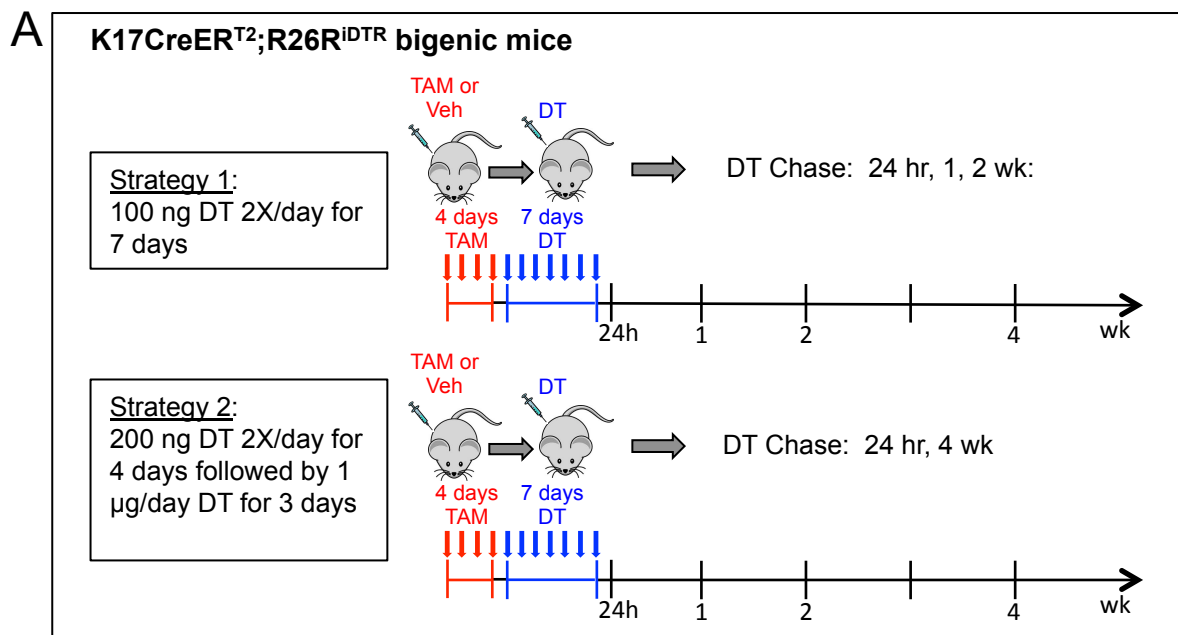


K17CreER^{T2};R26R^{EYFP} bigenic mice – TAM 24h chase





Legends to Supplemental Figures

Figure S1. Krt17 immunodetection in the TD and HF. Co-immunolabeling of Krt8 (A), Krt17 (B) in adult dorsal mouse skin sections detecting Krt17 in columnar keratinocytes in the TD but not in Krt8⁺ Merkel cells. White arrows indicate Krt17 labeling in the inner sheath (IS) of the infundibulum in primary guard (GHF) and secondary zig zag (ZHF) HFs. Krt17 immunolabeling is present in HF outer root sheath (ORS) cells although detection is weaker compared to IS cells. DAPI counterstain (blue) was conducted to visualize nuclei. Hashed lines demarcate the epidermal-dermal border. Abbreviation: epi, epidermis; der, dermis; MC, Merkel cell; TD, touch dome. Scale bar: 20 μ m.

Figure S2. Co-labeling of Krt17 and CD200 in the TD and generation of K17CreER^{T2} BAC transgenic mice. A, Co-immunolabeling of Krt17 (A), CD200 (B) in dorsal mouse skin sections. Krt17 is detected in columnar keratinocytes in the TD whereas CD200 is detected in the TD keratinocytes as well as in the Merkel cells (Woo et al., 2010). DAPI counterstain (blue) was conducted to visualize nuclei. Hashed lines demarcate the epidermal-dermal border. Brackets delineate TD area. Abbreviations: epi, epidermis; der, dermis; MC, Merkel cell. Scale bar: 20 μ m. B, schematic of the modified *Krt17* BAC (150 kB) with an inserted IRES-CreER^{T2} expression cassette in the 3' UTR of the mouse *Krt17* locus. The RP24-357E17 BAC was chosen as it contains 97.8 kB upstream and 51.5 kB downstream (gray boxes) of endogenous chromosome 11 sequence. Lower box shows the sequence of *Krt17* 3' UTR from the stop codon (red) to the poly A signal (underlined). Asterisk marks the IRES-CreER^{T2} insertion site (blue). C, micrograph of ethidium bromide-stained agarose gel detecting CreER^{T2} amplicons

confirming transmission of the K17CreER^{T2} BAC in pups from 1F3 and 1F4 founder mice. A wild-type gnDNA (Wt) and water control sample (C) is also shown. D, schematic for Cre recombination in Krt17⁺ cells (left), which induces EYFP expression in TAM-treated K17CreER^{T2};R26R^{EYFP} bigenic mice. Both 1F3 and 1F4 founder lines show equivalent levels of EYFP induction in TD keratinocytes (data not shown). Experimental design for genetic pulse chase studies in K17CreER^{T2};R26R^{EYFP} bigenic mice is shown on the right.

Figure S3. EYFP induction in K17CreER^{T2};R26R^{EYFP} mice and FACS protocol for isolation of TD keratinocytes from adult dorsal mouse skin. A-C, panoramic views of dorsal skin sections from K17CreER^{T2};R26R^{EYFP} mice harvested 24 hr post TAM and co-immunolabeled with Krt8, Krt17 and EYFP antibodies. Each panel illustrates co-labeling with either Krt8 and Krt17 (A), Krt8 and EYFP (B) or Krt8, Krt17 and EYFP (C) antibodies. Panel C demonstrates tight overlap between Krt17 immunolabeling and EYFP induction in the TD and HF ORS (arrows). Scale bar: 50 μ m. D-F, Schematic of the expression compartments for each surface protein (upper) are provided above their respective FACS dot plot (lower). D, FACS dot plots for α 6 integrin and CD34 to gate all proliferative keratinocytes. E, α 6⁺CD34⁺ gated cells (D) are analyzed for CD34 and Sca-1 levels, which allows for selection of Sca-1⁺ epidermal keratinocytes and exclusion of HF bulge cells (which also express CD200). F, α 6⁺CD34⁻Sca-1⁺ gated cells (E) are then analyzed for CD200 levels to select the CD200⁺ TD keratinocyte population.

Figure S4. Experimental strategy and utilization of K17CreER^{T2};R26R^{iDTR} mice. A, Schematic of the experimental design for genetic depletion of TDKCs in K17CreER^{T2};R26R^{iDTR} bigenic mice. B, FACS analysis of CD34⁺ HF bulge stem cells in K17CreER^{T2};R26R^{iDTR} mice showing a representative CD34 (y-axis) and Sca-1 (x-axis) scatter of control mouse epidermal cells containing a typical percentage of gated CD34⁺ bulge cells (left). On the right, comparison FACS plot of epidermal cells from K17CreER^{T2};R26R^{iDTR} mice 2 wk post TAM + DT. Note the approximate 80% depletion of bulge cells following DT treatment. C, Bar graph depicting the average percentage of TD stem cells in TAM + DT K17CreER^{T2};R26R^{iDTR} mouse skin compared to Veh + DT skin at 4 weeks following DT administration. Error bars show s.d.

Table S1. Microarray RNA profiling of FACS sorted TD $\alpha 6^+ \text{Sca-1}^+ \text{CD200}^+$ keratinocytes compared to the remainder of FACS-sorted $\alpha 6^+ \text{Sca-1}^+ \text{CD200}^-$ interfollicular epidermal (IFE) keratinocytes, Related to Figure 1.

Gene	CD200⁻ IFE abs. intensity	CD200⁺ TD abs. intensity	Fold increase in TD
<i>*Krt17</i>	43	344	8

*Microarray analysis of TD keratinocytes was previously published (Woo et al., 2010) and data have been deposited at Array Express with Accession Number E-MEXP-2925. Values for *Krt17* transcripts represent absolute intensities normalized to Gapdh levels ($p < 0.05$).

Table S2. Merkel cell counts performed for genetic pulse chase studies in K17CreER^{T2};R26R^{EYFP} mice, Related to Figures 1 and 2.

TAM chase	Number of mice	EYFP ⁺ Merkel cells	Total Merkel cells	Total TDs counted
24 hr	3	3	28	7
1 wk	3	28	75	11
3 wk	3	39	79	8
7 wk	3	73	92	13
12 wk	3	81	85	13

Table S3. Primer Sets Used in This Study, Related to Experimental Procedures.

Name	Sequence
pL451 Forward	5'-CTTCCCTCTCCGCTCCGGCATCACCCCTCCTGCTACAGCCTCT CCCCAGCATTCTATGCTTGAGACCATTAAAGCGTCGACGGGATC CGCCCCTCTCCCT-3'
pL451 Reverse	5'-CAGTCCACCTATTGTCACCATGGTCATTTATTTTCAGTGT TCAGAACAAGGCCACAGTTCACCTTCAGGTCAGCAAATTATG TACCTGACTGATGAAGTT-3'
Cre Forward	5'-GCGGTCTGGCAGTAAAACTATA-3'
Cre Reverse	5'-AGCGTTTTTCGTTCTGCCAAT-3'